Functional-Anatomic Fractionation of the Brain's Default Network

Jessica R. Andrews-Hanna,[1,2,5,*] Jay S. Reidler,[1] Jorge Sepulcre,[1,2,4] Renee Poulin,[1] and Randy L. Buckner[1,2,3,4]

[1]Department of Psychology and Center for Brain Science, Harvard University, Cambridge, MA 02138, USA
[2]Athinoula A. Martinos Center for Biomedical Imaging, Massachusetts General Hospital, Charlestown, MA 02129, USA
[3]Departments of Psychiatry and Radiology, Massachusetts General Hospital, Charlestown, MA 02129, USA
[4]Howard Hughes Medical Institute at Harvard University, Cambridge, MA 02138, USA
[5]Present address: Department of Psychology and Neuroscience, University of Colorado at Boulder, Boulder, CO 80309, USA
*Correspondence: jessica.andrews-hanna@colorado.edu
DOI 10.1016/j.neuron.2010.02.005

SUMMARY

One of the most consistent observations in human functional imaging is that a network of brain regions referred to as the "default network" increases its activity during passive states. Here we explored the anatomy and function of the default network across three studies to resolve divergent hypotheses about its contributions to spontaneous cognition and active forms of decision making. Analysis of intrinsic activity revealed the network comprises multiple, dissociated components. A midline core (posterior cingulate and anterior medial prefrontal cortex) is active when people make self-relevant, affective decisions. In contrast, a medial temporal lobe subsystem becomes engaged when decisions involve constructing a mental scene based on memory. During certain experimentally directed and spontaneous acts of future-oriented thought, these dissociated components are simultaneously engaged, presumably to facilitate construction of mental models of personally significant events.

INTRODUCTION

When individuals are left to think to themselves undisturbed, a specific network of brain regions becomes engaged. This network, referred to as the default network, was originally observed during passive, experimental control tasks that were included in a variety of studies (Shulman et al., 1997; Mazoyer et al., 2001). Raichle and colleagues (Raichle et al., 2001; Gusnard and Raichle, 2001) drew attention to the network and suggested that its ubiquitous appearance in default states signals an essential, adaptive function. The network has since received growing attention because of its alteration in neurological and psychiatric disorders (Buckner et al., 2008; Broyd et al., 2009). However, despite the widespread interest there has not been consensus on the default network's functions or even whether its presence signifies an adaptive contribution to cognition (Gilbert et al., 2007; Morcom and Fletcher, 2007). The present series of studies

sought to resolve these discrepancies by dissecting its anatomy and function.

Possible functions of the default network are suggested by two sources of evidence. The first source comes from studies of directed tasks that cause activity increases in regions within the default network. Anatomically, the default network comprises regions along the anterior and posterior midline, the lateral parietal cortex, prefrontal cortex, and the medial temporal lobe (Buckner et al., 2008). Tasks that encourage subjects toward internal mentation, including autobiographical memory, thinking about one's future, theory of mind, self-referential and affective decision making, tend to activate regions within the default network (reviewed in Ochsner et al., 2004; Buckner et al., 2008; Spreng et al., 2009).

A challenge to the field has been to disentangle such high-level tasks into component processes. Some have suggested a role for components of the default network in scene construction (Hassabis and Maguire, 2007), contextual associations (Bar, 2007), and conceptual processing (Binder et al., 2009). Others have suggested a role for the default network in social (Mitchell, 2006; Schilbach et al., 2008), self-referential, or affective cognition (Gusnard et al., 2001; Wicker et al., 2003; D'Argembeau et al., 2005, 2009) with minimal emphasis on mnemonic or prospective processes (but see D'Argembeau et al., 2009). Schacter and Addis (2007) highlighted that future-oriented thoughts, which strongly drive activity in the default network, are inherently constructive, building on multiple episodic memories. They further argued that mental simulation based on memory is a core process of future-oriented cognition (Schacter et al., 2007). The divergence across these perspectives, perhaps exemplified best by the different emphases in Hassabis and Maguire's scene construction model (Hassabis and Maguire, 2007) and D'Argembeau et al.'s emphasis on self-referential cognition (D'Argembeau et al., 2005, 2009), suggests that the default network likely comprises multiple interacting subsystems (e.g., Hassabis et al., 2007a; Buckner et al., 2008).

The second source of evidence about the function of the default network comes from examination of what people think about during passive task states. Associations between default network activity and spontaneous thoughts have emerged in multiple studies (e.g., McKiernan et al., 2006; Mason et al., 2007; Christoff et al., 2009). In terms of content, individuals report spontaneously thinking about personally significant or

concerning events (Singer, 1966; Klinger, 1971), a considerable portion of which possess a future orientation (Andreasen et al., 1995; J.R.A.-H. and R.L.B., unpublished data). Other researchers have emphasized the social aspects of spontaneous thought (Mitchell, 2006; Schilbach et al., 2008). Despite these observations, it remains unclear why the specific regions within the default network activate together during passive epochs and how they might support the kinds of internal mentation reported by participants.

In this paper, we conducted a detailed characterization of the architecture of the default network using analysis of intrinsic connectivity combined with graph-analytic and clustering techniques. Next, task-based functional MRI (fMRI) was employed to explore the differential contributions of the component systems comprising the default network. Participants made decisions about themselves in the future with task variations constructed to manipulate self-referential processing and the demands for de novo construction of an imagined scene. As the results will reveal, the task variations differentially modulated distinct components of the default network. We further examined the functions of the dissociated components by exploring the nature of strategies used during each task trial. These dissociated components contribute differentially to two processes common during spontaneous thought: construction of imagined events and assessment of their personal significance.

RESULTS

Experiment 1
The Default Network Comprises Two Subsystems that Interact with a Common Core
In order to characterize the architecture of the default network, intrinsic functional connectivity MRI (fcMRI) was used to extract low-frequency spontaneous blood oxygenation level-dependent (BOLD) fluctuations within 11 a priori midline and lateral regions within the default network (Figures 1A and 1B; Table S1). The fluctuations within the a priori regions were then examined in an independent group of young adults using graph-analytic techniques and hierarchical clustering analysis on the interregional correlation matrix.

Results revealed that the default network comprises a large-scale interacting brain system—no single region was completely dissociated from the remaining regions. However, local structure that was not captured by considering it as a single, coherent system was also apparent. Graph-analytic techniques revealed a core set of hubs, including posterior cingulate cortex (PCC) and anterior medial prefrontal cortex (aMPFC), defined by their significant (p < 0.001) correlations with all regions comprising the network (Figure 1C). Consistent with prior reports (Buckner et al., 2009; see also Hagmann et al., 2008), PCC and aMPFC exhibited the highest betweenness centrality. Hierarchical clustering analysis on the remaining nine regions within the default network revealed that they dissociated into two distinct subsystems (Figure 1D). One subsystem, termed the "dorsal medial prefrontal cortex (dMPFC) subsystem," included the dMPFC, temporoparietal junction (TPJ), lateral temporal cortex (LTC), and temporal pole (TempP). The second subsystem, termed the "medial temporal lobe (MTL) subsystem," included the ventral MPFC (vMPFC),

posterior inferior parietal lobule (pIPL), retrosplenial cortex (Rsp), parahippocampal cortex (PHC), and hippocampal formation (HF[+]).

These initial results suggest that the default network is a heterogeneous brain system comprised of at least two distinct subsystems that interact with a core set of hubs. The next two experiments sought to provide insight into the distinct functional contributions of each component of the default network.

Experiment 2
The Default Network Subsystems Functionally Dissociate
The second experiment explored the functional response properties of the core and subsystems identified in experiment 1 using an fMRI paradigm that allowed prospective, episodic decisions about one's self (*Future Self*) to be compared to self-referential decisions concerning one's present situation or mental state (*Present Self*). Based on prior findings from memory and social cognitive neuroscience studies, we hypothesized that while both conditions might activate the midline core, the *Future Self* condition would preferentially activate the MTL subsystem, and the *Present Self* condition would preferentially activate the dMPFC subsystem. Additionally, the two experimental conditions were referenced to parallel control conditions that relied on nonpersonal semantic knowledge (*Future Non-Self Control* and *Present Non-Self Control*). Thus, the 2 × 2 Self-Relevancy (*Self*, *Non-Self Control*) × Temporal Orientation (*Present*, *Future*) experimental paradigm allowed us to examine how distinct processes differentially map onto the default network components.

Behavioral Results. Behavioral strategy probes obtained immediately following the scanning session confirmed that the conditions differed as expected. Large differences in participants' sense of self-projection were observed between the *Self* and *Non-Self* (semantic) *Control* conditions (*Present Self* = 5.22 ± 0.39; *Present Non-Self Control* = 1.77 ± 0.46; *Future Self* = 6.88 ± 0.23; *Future Non-Self Control* = 1.93 ± 0.27). These differences yielded significant main effects (Self-Relevancy: $F(1,17) = 190.8$, p < 0.001; Temporal Orientation: $F(1,17) = 27.4$, p < 0.001) and a significant interaction ($F(1,17) = 7.6$, p < 0.05). Differences were also observed in participants' reported use of mental imagery (*Present Self* = 5.82 ± 0.32; *Present Control* = 5.37 ± 0.33; *Future Self* = 7.28 ± 0.25; *Future Control* = 4.80 ± 0.27). Specifically, there was a significant main effect ($F(1,17) = 10.0$, p < 0.005) with mental imagery rated stronger for the two *Self* conditions, no main effect of Temporal Orientation ($F(1,17) = 2.0$, p = 0.18), and a significant interaction ($F(1,17) = 15.8$, p < 0.001). Vividness ratings paralleled mental imagery and also varied across conditions. A main effect of Self-Relevancy ($F(1,17) = 11.0$, p < 0.005), no main effect of Temporal Orientation ($F(1,17) = 1.35$, p = 0.26), and a significant interaction ($F(1,17) = 8.76$, p < 0.01) was observed.

Of note, the *Future Self* condition showed the highest levels of self-projection, experienced mental imagery, and vividness, suggesting that thinking about oneself in the future may simultaneously engage a number of component processes subserved by subsystems that comprise the default network. This observation provides an important clue about why constructed thoughts about one's future may activate such a widely distributed set of
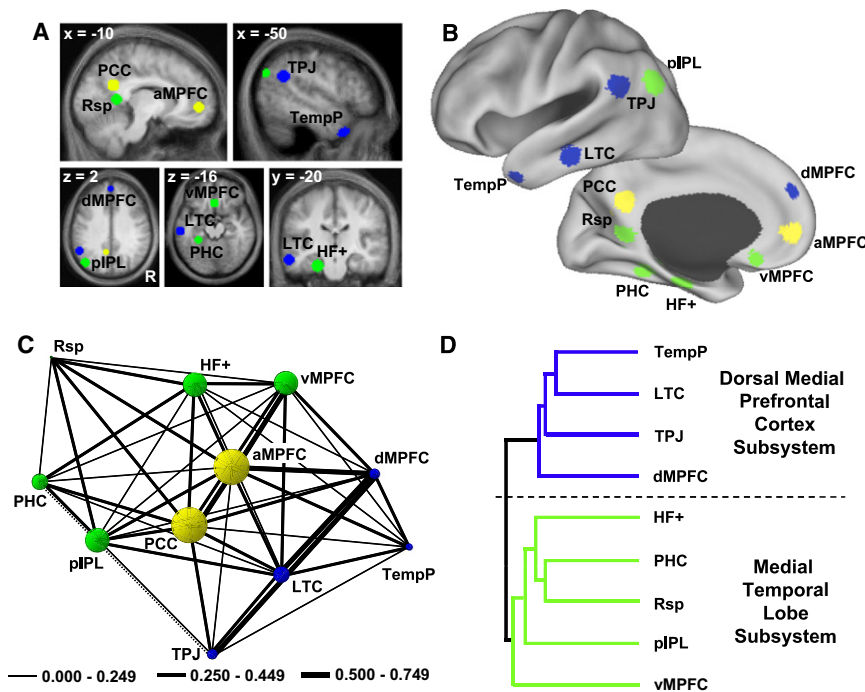
Figure 1. Intrinsic Functional Connectivity Reveals that the Default Network Is Comprised of a Midline Core and Two Distinct Subsystems

(A) Eleven a priori regions within the default network were defined using low-frequency intrinsic connectivity approaches in a group of 28 adults. The regions are shown overlain on transverse slices colored according to the subsystems revealed in (C) and (D).

(B) Regions are also projected onto a surface template (Caret software, Van Essen, 2005).

(C) Functional correlation strengths between the 11 regions were extracted in an independent sample of participants and examined for clustering properties using the Kamada-Kawai algorithm, which pulls strongly correlated regions near each other and pushes weakly correlated regions farther apart. The thickness of the lines reflects the strength of the correlation between regions. The dotted line demonstrates a negative correlation. Only significant correlations at p < 0.001 are included in the analysis. The size of the circles represents a measure of betweenness-centrality, a graph-analytic metric that rep-resents how central a node is in a network (see text). The two regions with the highest betweenness-centrality are anterior medial prefrontal cortex (aMPFC) and posterior cingulate cortex (PCC), reflecting a core set of "hubs" within the default network (colored yellow accordingly).

(D) Hierarchical clustering analysis was performed to investigate whether the remaining regions with more limited connectional properties grouped into distinct subsystems. Two clusters representing subsystems emerged. The first subsystem (colored in blue and referred to as the "dorsal medial prefrontal cortex subsystem") included dorsal medial prefrontal cortex (dMPFC), temporoparietal junction (TPJ), lateral temporal cortex (LTC), and temporal pole (TempP). The second subsystem (colored in green and referred to as the "medial temporal lobe subsystem") included ventral MPFC (vMPFC), posterior inferior parietal lobule (pIPL), retrosplenial cortex (Rsp), parahippocampal cortex (PHC), and hippocampal formation (HF+).

brain regions. Experiment 3 will expand upon this observation by considering the differential use of strategies across conditions and whether their use tracks functional-anatomic distinctions between default network components.

A one-way repeated-measures ANOVA revealed that conditions varied significantly with respect to response time (RT) ($F(3,51) = 8.12$, p < 0.001; *Present Self* = 5696 ms ± 179 ms; *Present Non-Self Control* = 6642 ms ± 125 ms; *Future Self* = 6185 ms ± 147 ms; *Future Non-Self Control* = 6500 ms ± 160 ms), a variable that has been shown to influence activity within the default network (e.g., McKiernan et al., 2003). In order to ensure that differences in activation patterns between the conditions were not simply the result of RT differences, all regional analyses were computed after controlling for this measure. Specifically, we performed a linear regression between the group-averaged percent signal change on a trial-by-trial basis (dependent measure) and the group-averaged RT on a trial-by-trial basis (independent measure) and saved the residuals for subsequent analyses. For this reason, when viewing the figures, the sign of the percent signal change should not be interpreted because the residuals sum to zero.

Imaging Results. The mean activity (representing percent signal change after controlling for RT) was computed by averaging the percent signal change across the regions comprising the core as well as each of the two subsystems (Figure 2). Three distinct patterns emerged consistent with our hypotheses. The

core showed strong activation in both conditions where subjects made autobiographical (*Self*) decisions (Figure 2A). The two subsystems, however, showed selective activation increases. The dMPFC subsystem was preferentially engaged when participants made self-referential judgments about their present situation or mental states (Figure 2B), whereas the MTL subsystem was preferentially engaged during episodic judgments about the personal future (Figure 2C). These observations were all confirmed by statistical tests (see Table S2).

Preliminary insight into the processing contributions of one of the subsystems was revealed by trial-to-trial variance in imagery ratings. Ratings of visual imagery correlated with activity in the MTL subsystem ($r(70) = 0.39$, p < 0.005, significant at a Bonferroni-corrected α of 0.008) but not significantly for the core ($r(70) = 0.19$, p = 0.11) or the dMPFC subsystem ($r(70) = 0.00$, p = 0.98). Thus, trials rated as eliciting appreciable amounts of visual imagery tended to be associated with greater activity within the MTL subsystem. Additionally, ratings of self-projection strongly correlated with fMRI activity in the MTL subsystem and the core and marginally in the dMPFC subsystem (dMPFC: $r(70) = 0.22$, p = 0.06; MTL: $r(70) = 0.38$, p < 0.001; core: $r(70) = 0.313$, p < 0.01; the MTL and core were both significant at a Bonferroni-corrected α of 0.008). Note that estimated use of imagery and self-projection were not independent, even when variance within a condition was examined. For example, imagery and self-projection estimates were highly correlated across
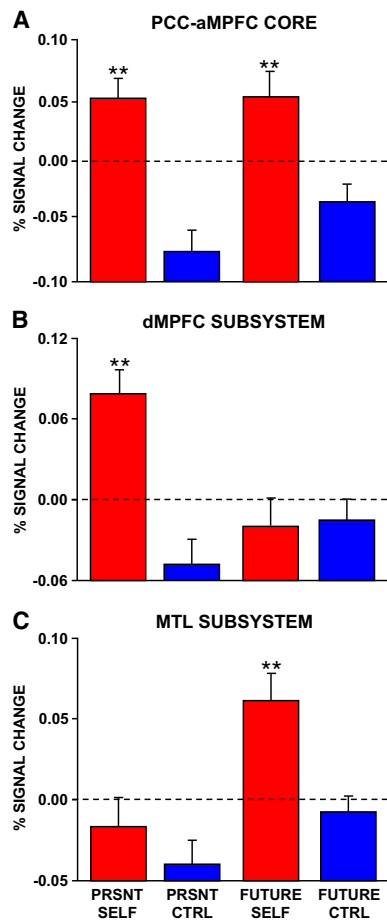
Figure 2. Functional Dissociation of Default Network Components

Percent signal change controlled for trial-by-trial differences in response time is plotted for each condition within the core and the two subsystems as defined by intrinsic connectivity analysis in Figure 1.

(A) The mean activity within the regions comprising the core exhibits a main effect of *Self > Non-Self Control* trials, but no difference based on temporal context. Functional task dissociations were revealed for the subsystems comprising the default network.

(B) The dMPFC subsystem is preferentially activated when participants make self-referential decisions about their present situation or mental states.

(C) In contrast, the MTL subsystem exhibits preferential activity when participants make decisions about their personal future. Note that since the activity magnitudes were controlled for RT, the zero value and +/− sign are relative. Axes are plotted to maintain visual consistency across figures. PRSNT SELF, present self; PRSNT CTRL, present non-self control; FUTURE CTRL, future non-self control. Error bars represent standard error of the mean.

individual trials within the *Future Self* condition (r = 0.81). These correlations, however, suggested to us a way to gain insight into the component processing contributions of the functional-anatomical components. We will return to analysis of correlations between subsystem activity and reported strategy use in experiment 3.

Exploratory Whole-Brain Analyses Confirm Functional Dissociation

The above analyses demonstrate a compelling dissociation between the core and subsystems within the larger default network. To further explore these dissociations, we analyzed the critical contrasts at a map-wise level without making assumptions about the architecture of the default network. Such exploratory analyses provide an independent means of describing functional differences. Two contrasts were explored: *Self* versus *Non-Self Control* and *Future Self* versus *Present Self*. The first contrast isolates those regions preferentially activated by tasks involving referencing information to one's self, whereas the second contrast selectively isolates differences between the two self-referential conditions.

Results revealed increased activity notably within the aMPFC and PCC core regions for the *Self* compared to *Non-Self Control* conditions. In addition, several regions that fell within both subsystems were also activated by the main effect contrast, including dMPFC, TPJ, pIPL, Rsp, and TempP (Figure 3). The contrast between the two *Self* conditions confirmed the dissociation between the two subsystems observed in the ROI analyses with a particularly clean isolation of the MTL subsystem. As highlighted in Figure 4, the regions that preferentially activate during self-relevant predictions about one's future nearly identically (and selectively) overlap the regions that define the MTL subsystem. These regions include bilateral vMPFC, Rsp, pIPL, PHC, and HF[+]. In contrast, regions comprising the dMPFC subsystem were more active during decisions about one's present situation or mental state (dMPFC, TPJ, TempP), although a number of additional regions associated with a frontoparietal control system (bilateral middle/superior frontal gyrus, right ventrolateral PFC, bilateral insula, anterior cingulate cortex, and anterior inferior parietal sulcus) were also observed. Taken collectively, these results confirm the dissociations observed in the hypothesis-driven contrasts with particularly strong evidence for the core and MTL subsystem.

Item-Analysis Confirms Functional Dissociation

The results of the intrinsic connectivity analysis suggest that the default network clusters into two distinct subsystems, with strong intrinsic correlations between the individual regions comprising each subsystem. Our next objective was to examine whether regions within each subsystem track together during task performance. If so, these results would provide additional support for the presence of subsystems within the default network. To investigate these questions, the mean percent signal change for the four conditions was plotted separately for each region comprising the distinct subsystems. Regions comprising the same subsystems exhibit very similar patterns of activity, while regions comprising distinct subsystems exhibit relatively different patterns of activity (Figures S1 and S2).

Next, we took advantage of the study's large sample size to estimate trial-by-trial activity magnitudes independent of condition and to calculate interregional activity correlations. The degrees to which individual subsystem regions correlated with other regions within the same subsystem (e.g., PHC with pIPL), with the core regions (e.g., PHC with aMPFC), and with the regions comprising distinct subsystems (e.g., PHC with dMPFC) were all quantified. Consistent with the intrinsic activity correlations in experiment 1, the mean trial-by-trial activity correlation between all pairs of regions comprising each subsystem (n = 16 pair-wise correlations) was strong (Figure 5A; mean r = 0.45, one-sample t test: t(15) = 7.98, p < 0.001, significant

SELF > CONTROL

z = 40   z = 25   z = 10   z = -5   z = -20

R

p < 10⁻⁴   p < 10⁻¹²
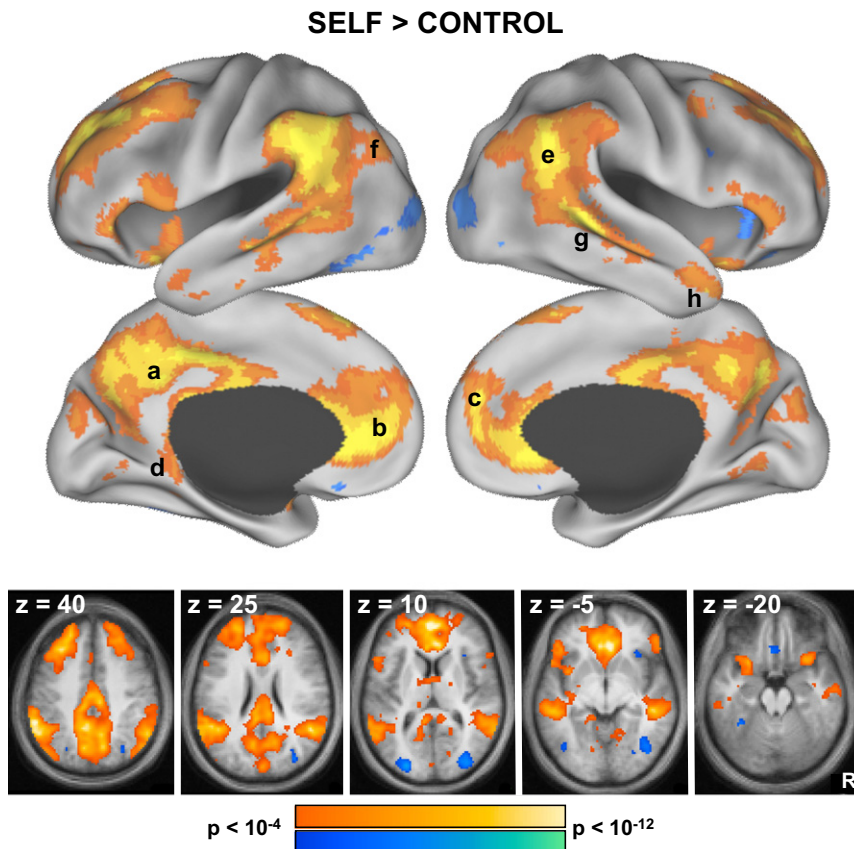
Figure 3. Whole-Brain Analyses Reveal the Role of the Midline Core in Self-Referential Processing

Whole-brain exploratory analyses were conducted using the main effect contrast of *Self* trials versus *Non-Self Control* trials. Results are projected onto a surface template (Caret software; Van Essen, 2005) and are also illustrated in slices (both, p < 0.0001 uncorrected). Warm colors represent greater activation during *Self* trials, whereas cool colors represent greater activation during *Non-Self Control* trials. Increased activation during *Self* trials was observed prominently in (A) PCC and (B) aMPFC cores, as well as in (C) dMPFC, (D) Rsp, (E) TPJ, (F) pIPL, (G) LTC, and (H) TempP.

Collectively, these results indicate that regions comprising the subsystems and core act as functionally coherent units during task performance, exhibiting both correlation and independence as predicted by the analyses in experiment 1.

Experiment 3
Analysis of Component Processes Supported by the Core and Subsystems

To gain insight into the component processes supported by the dissociated network components, including how they might combine together during certain 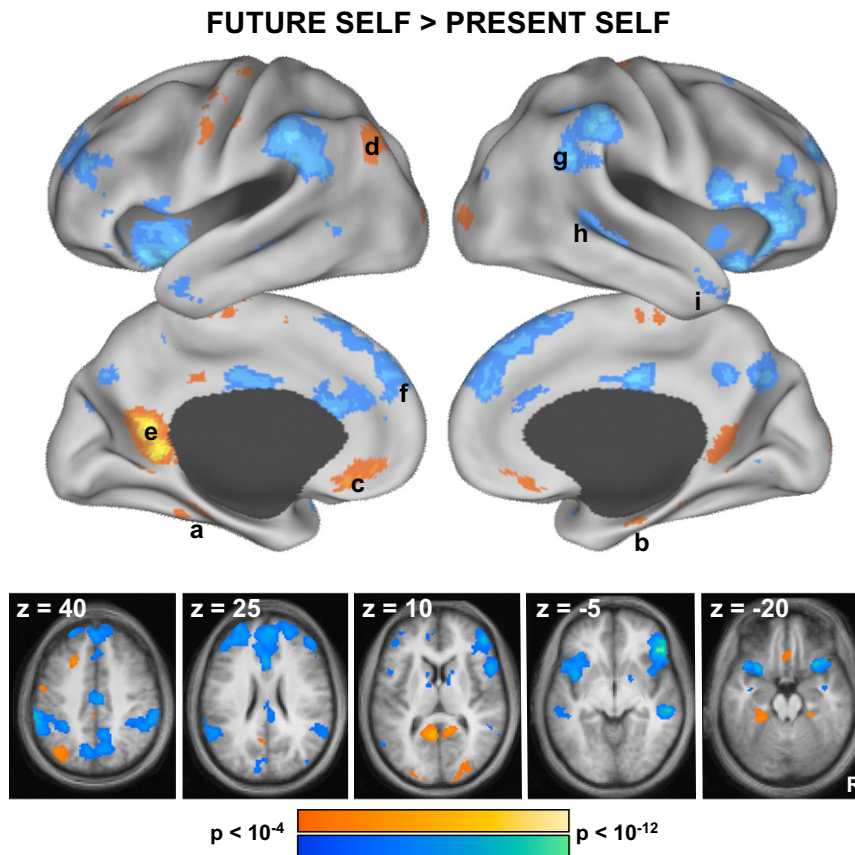forms of experimentally directed and passive tasks, the third experiment conducted a detailed analysis of the reported strategies that tracked activity differences. Specifically, we examined the reported strategies used for each of the questions in relation to the evoked activity to better understand the nature of the supported processes.

Strategy probes were diverse and examined a range of possible component strategies, including whether individual trials relied on episodic memory, use of imagination, specific mental images that involved scenes, affective content including feelings and emotions, and self-referenced ideations. Several results from the strategy probes confirmed expected differences between the conditions, bolstering confidence in the approach (see Table S3 for ratings). For example, strategy probe #8 asked to what degree participants thought about the future while answering the questions. As expected, responses were considerably higher for the future-oriented conditions (*Future Self* and *Future Non-Self Control*). Strategy probe question #11 asked about the overall effort exerted to answer the questions. The reported subjective responses paralleled the response time differences observed between conditions (with the two *Control* conditions showing the greatest effort). Additionally, strategy probe #9 asked whether factual as opposed to subjective information was relied upon when answering the questions. Both of the *Non-Self Control* conditions showed the highest factual response properties consistent with their focus on general semantic knowledge.

at a Bonferroni corrected α of 0.01). Similarly, the mean correlation between each region comprising the two subsystems and the two regions comprising the core (n = 18 pair-wise correlations) was also strong, confirming the role of the core as hubs within the default network (mean r = 0.31, one-sample t test: $t(17)$ = 9.21, p < 0.001). In contrast, pair-wise correlations between regions comprising distinct subsystems (n = 20 pair-wise correlations) were near zero, highlighting the distinct nature of the two subsystems (mean r = 0.05, one-sample t test: $t(19)$ = 1.19, p = 0.25). Finally, the two regions comprising the core were strongly correlated with each other (aMPFC with PCC: $r(70)$ = 0.61, p < 0.001).

Next, the interregional activity correlation matrix (9 × 9) between all pairs of regions calculated above (minus the hubs) was analyzed using hierarchical clustering to examine shared task-related variance between the regions in a data-driven manner. Mirroring the intrinsic connectivity results from experiment 1, the dMPFC, TPJ, LTC, and TempP and the vMPFC, pIPL, Rsp, PHC, and HF formed distinct clusters (Figure 5B). The regions within the MTL subsystem exhibited the identical pattern as revealed by intrinsic connectivity (compare Figure 1D to 5B), whereas the regions within the dMPFC subsystem clustered together but showed a different organizational structure. Whereas intrinsic connectivity grouped the LTC and TempP closest to one another within the dMPFC subsystem, the LTC exhibited task-related activity that correlated best with the TPJ.
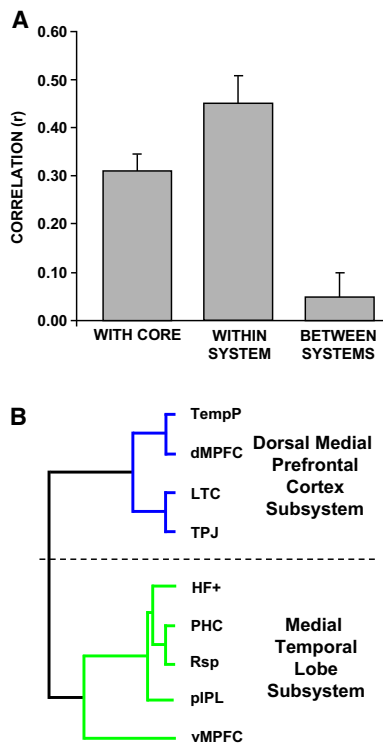
FUTURE SELF > PRESENT SELF

Whole-brain exploratory analyses were conducted using the simple effect contrast *Future Self* versus *Present Self*, projected onto a surface template and illustrated in slices (both, p < 0.0001 uncorrected). Warm colors represent greater activation during *Future Self* trials, whereas cool colors represent greater activation during *Present Self* trials. Increased activation during *Future Self* trials was observed selectively in regions comprising the MTL subsystem, including bilateral (A) PHC, (B) HF$^+$, (C) vMPFC, (D) pIPL, and (E) Rsp. In contrast, a number of regions within and outside the dMPFC subsystem were recruited more during *Present Self* trials: i.e., (F) dMPFC, (G) TPJ, (H) LTC, and (I) TempP. Note the lack of difference between the two conditions was observed in the PCC and the aPFC core regions.

Three distinct strategy probes tracked the observed activity increases in the MTL subsystem: use of episodic memory (probe #5), event imagination (probe #6), and scene content (probe #7). As shown in Figures 6D–6F, ratings across the three strategy probes showed no Strategy × Self-Relevancy × Time interaction ($F(1,11) = 0.23$, p = 0.80), a significant Self-Relevancy × Temporal Orientation interaction ($F(1,11) = 6.47$, p < 0.05), a significant main effect of Self-Relevancy ($F(1,11) = 5.36$, p < 0.05), and a significant main effect of Temporal Orientation (*Future* versus *Present*: $F(1,11) = 24.5$, p < 0.001). All three variables were rated stronger for the *Future Self* condition than the *Present Self* condition, similar to the observed activity pattern within the MTL subsystem (see Figure 2C). Note that this pattern is dissociated from that observed for the Affective Self-Referential composite, which is characterized by marked activity increases in both of the *Self* conditions. When the three strategy probes were combined into a composite—which we descriptively label the "Mnemonic Scene Construction" composite—the composite measure accounted for 31% of the variance in MTL subsystem activity ($r(64) = 0.56$, p < 0.001, significant at a Bonferroni corrected α of 0.008; Figure 7F), but only 3% of the variance in activity within the midline core ($r(64) = 0.17$, p = 0.16; Figure 7D) and 3% of the variance in the dMPFC subsystem ($r(64) = -0.17$, p = 0.18; Figure 7E).

These results suggest that the core and MTL subsystem contribute to distinct component processes that are differentially linked to self-referential processing and memory-based scene construction, respectively. Recognizing that these strategy probes capture only broad sets of processes that must be dissected further, it is notable that the distinct neural components of the default network so clearly tracked the dissociated component processes. Thinking about one's self in the future, which was characterized by extensive use of self-referential

Beyond these expected results, a subset of the strategy probes resulted in informative response patterns that tracked activity in the core and the MTL subsystem (Figure 6). Three specific strategy probes strongly tracked the observed activity increases in the aMPFC and PCC core: personal significance (probe #1), introspection about one's preferences, feelings, and emotions (i.e., mental states) (probe #2), and evoked emotion (probe #3) (Figures 6A–6C). Across the three strategy probes, ratings showed no Strategy × Self-Relevancy × Temporal Orientation interaction ($F(2,22) = 0.68$, p = 0.52), no Self-Relevancy × Temporal Orientation interaction ($F(1,11) = 0.31$, p = 0.59), a significant main effect of Self-Relevancy ($F(1,11) = 39.6$, p < 0.001), and no main effect of Temporal Orientation ($F(1,11) = 0.028$, p = 0.87). Thus, the three strategy probes were similarly rated as higher for both *Self* conditions. When the three variables were combined into a composite measure—which we descriptively label the "Affective Self-Referential" composite—the composite variable accounted for 22% of the trial-to-trial variance in activity within the midline core ($r(64) = 0.47$, p < 0.001, significant at a Bonferroni corrected α of 0.008; Figure 7A). The Affective Self-Referential composite also explained a considerable portion (13%) of the variance in activity within the dMPFC subsystem ($r(64) = 0.36$, p < 0.005, also significant at a Bonferroni corrected α of 0.008; Figure 7B) and only 5% of the variance in activity within the MTL subsystem ($r(64) = 0.23$, p = 0.06; Figure 7C).

Figure 5. Interregional Correlation and Clustering Analyses Confirm Functional Dissociation

Large sample sizes permit reliable estimates of trial-by-trial activity collapsing across conditions.

(A) Activity within each region comprising the subsystems defined from intrinsic connectivity analysis was extracted and correlated with activity within each of the hubs. The correlation values between each region and the two core hubs were then averaged (left bar). Likewise, activity correlations between regions comprising the same subsystem were averaged to reflect within-subsystem correlations (middle bar). Finally, activity correlations between regions comprising distinct subsystems were averaged to reflect between-subsystem correlations (right bar). Robust correlations were observed between regions within subsystems and between subsystems and the hubs. However, regions belonging to distinct subsystems exhibited minimal task-related activity correlations.

(B) Hierarchical clustering analysis on the correlation matrix between trial-by-trial activity in each region was conducted using identical methods as in Figure 1D to examine whether the regions dissociate functionally during tasks. Two distinct clusters were revealed, suggesting that regions within each subsystem exhibit similar patterns of activity but overall different patterns from the other subsystem. Note that the cluster analysis reveals a very similar clustering pattern between the regions comprising the MTL subsystem as illustrated in Figure 1D. However, the regions comprising the dMPFC subsystem exhibited clustering patterns that were different from that revealed by intrinsic connectivity analysis.

Error bars represent standard error of the mean.

processing and concurrent processes associated with constructing a mental scene based on memory, maximally activated both the core and the MTL subsystem.

DISCUSSION

Originally observed in meta-analyses of passive task data (Shulman et al., 1997; Mazoyer et al., 2001), the default network has

received considerable attention because of the possibility that it participates in important functions that reflect more than a quiescent or idling brain state (Raichle et al., 2001; Gusnard and Raichle, 2001). Among multiple possibilities, a reemerging theme is that the default network contributes to internal mentation that becomes prominent when people are not engaged in external interactions and their minds wander (Buckner et al., 2008). Foreshadowed by William James, such "stream of thought" may reflect what we do the majority of the time (James, 1890; Klinger and Cox, 1987), likely signaling important adaptive functions (Singer, 1966; Klinger, 1971). The nature of the default network's contribution to adaptive function, however, has been widely debated. While some theories emphasize its role in construction of a mental scene (Hassabis and Maguire, 2007), other theories emphasize self-referential or social processes (Wicker et al., 2003; Mitchell, 2006; D'Argembeau et al., 2005; Schilbach et al., 2008). Our results reveal that both of these theories are correct but account for distinct functional-anatomic components within the default network. Moreover, the present set of analyses show how each component may contribute to processes common during spontaneous thought.

The Default Network Consists of a Midline Core and Distinct Subsystems

The default network is comprised of two distinct subsystems that converge on a midline core (Figures 1 and 5). Functional connectivity combined with network and hierarchical clustering analysis revealed a tightly correlated MTL subsystem comprising the HF⁺, PHC, Rsp, vMPFC, and pIPL and a distinct dMPFC subsystem comprising the dMPFC, TPJ, LTC, and TempP. Importantly, both subsystems strongly correlated with a midline core that included the aMPFC and PCC. Before suggesting functional attributes for the distinct components, we first discuss the convergence between the present results and prior functional connectivity and connectional anatomy studies.

The macaque medial temporal lobe is anatomically connected to the Rsp (Kobayashi and Amaral, 2003, 2007), the ventral-caudal mPFC (Barbas et al., 1999; Kondo et al., 2005), and the lateral parietal area 7a—the possible macaque homolog of human pIPL (Suzuki and Amaral, 1994; Lavenex et al., 2002). Using fcMRI in humans, we previously demonstrated that the HF⁺ is intrinsically correlated with a similar set of regions, including pIPL, Rsp, and vMPFC (Vincent et al., 2006; Kahn et al., 2008; see also Greicius et al., 2004) and similar patterns of connectivity have been found when examining intrinsic correlations with the vMPFC and Rsp (Margulies et al., 2007, 2009).

The PCC and the aMPFC comprise a core within the default network, and their widespread connectivity is supported by connectional anatomy studies. In macaques, PCC exhibits strong reciprocal connections with many of the regions comprising both subsystems: PHC, HF⁺, Rsp, MPFC, and LTC (Barbas et al., 1999; Kobayashi and Amaral, 2003, 2007; Morecraft et al., 2004). The aMPFC (area 10) is also strongly connected with a number of medial prefrontal and posterior regions, including ventral and dorsal MPFC, PCC, Rsp, LTC, and TempP (Barbas et al., 1999; Price, 2007). We recently demonstrated using unbiased voxel-wise intrinsic connectivity methods that both the PCC and the aMPFC are "hubs" exhibiting high levels
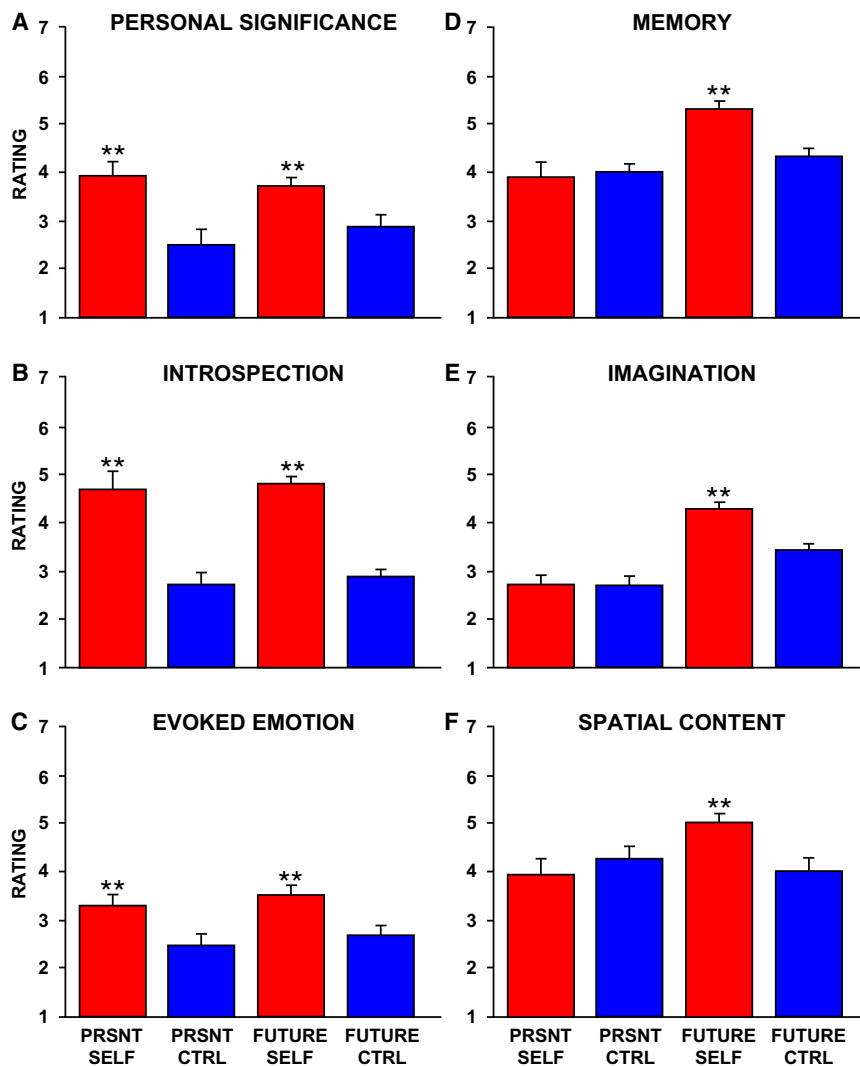
Figure 6. Assessment of Strategy Use Reveals Multiple Component Processes

To further explore the component processes eliciting activity in the default network, an independent sample of participants rated each stimulus on a number of dimensions using a seven-point Likert scale (1, not at all; 7, a lot). Three variables capture the distinction between *Self* and *Non-Self Control* trials, exhibiting patterns similar to the core in Figure 2A: (A) personal significance, (B) introspection, and (C) evoked emotion. However, these variables do not account for the difference in activity observed between *Future Self* and *Present Self* trials. In contrast, three additional variables yielded patterns similar to task-related brain activity within the MTL subsystem as highest for Future Self trials (Figure 1B). These variables include (D) memory, (E) imagination, and (F) spatial content. PRSNT SELF, present self; PRSNT CTRL, present non-self control; FUTURE CTRL, future non-self control. Error bars represent standard error of the mean.

activation during remembering and prospection implies that a common set of processes underlies these abilities. Employing strategy probes and item analysis, our results revealed that participants used a strategy that involved constructing a mental scene based on memory. This mnemonic scene construction strategy explained 32% of the variance in activity within the MTL subsystem, suggesting that mnemonic scene construction is an important component process of thinking about the future (Hassabis and Maguire, 2007). Of importance, this set of processes is selectively supported by the MTL subsystem and not by all components of the default network.

The present results also hint at the possibility that the MTL subsystem is more sensitive to the act of simulating the future using mnemonic imagery-based processes than to temporal aspects of the future per se. In particular, although the relationship between activity within the MTL subsystem and future thinking (item ratings for question #8 in Table S1) was robust and significant ($r = 0.68$), it reduced to near zero ($r = 0.03$) when controlling for the effect of mnemonic scene construction. Consistent with this finding, patients with hippocampal amnesia lack the ability to imagine a coherent scene presumably void of a temporal context (Hassabis et al., 2007b; see also Hassabis et al., 2007a; Addis et al., 2009). Because participants are more likely to take part in future events that are simulated with greater contextual detail compared to those imagined abstractly (Gollwitzer and Brandstaetter, 1997), we suspect that the adaptive significance of these mnemonic imagery-based processes may be to benefit prediction accuracy and future behavior.

of distributed functional connectivity throughout the cortex (Buckner et al., 2009; see also Hagmann et al., 2008). The PCC, in particular, correlates with all regions that fall within the default network, even after taking the correlation between other default network regions into account (Fransson and Marrelec, 2008).

The Default Network Components Exhibit Distinct Functional Contributions to Cognition
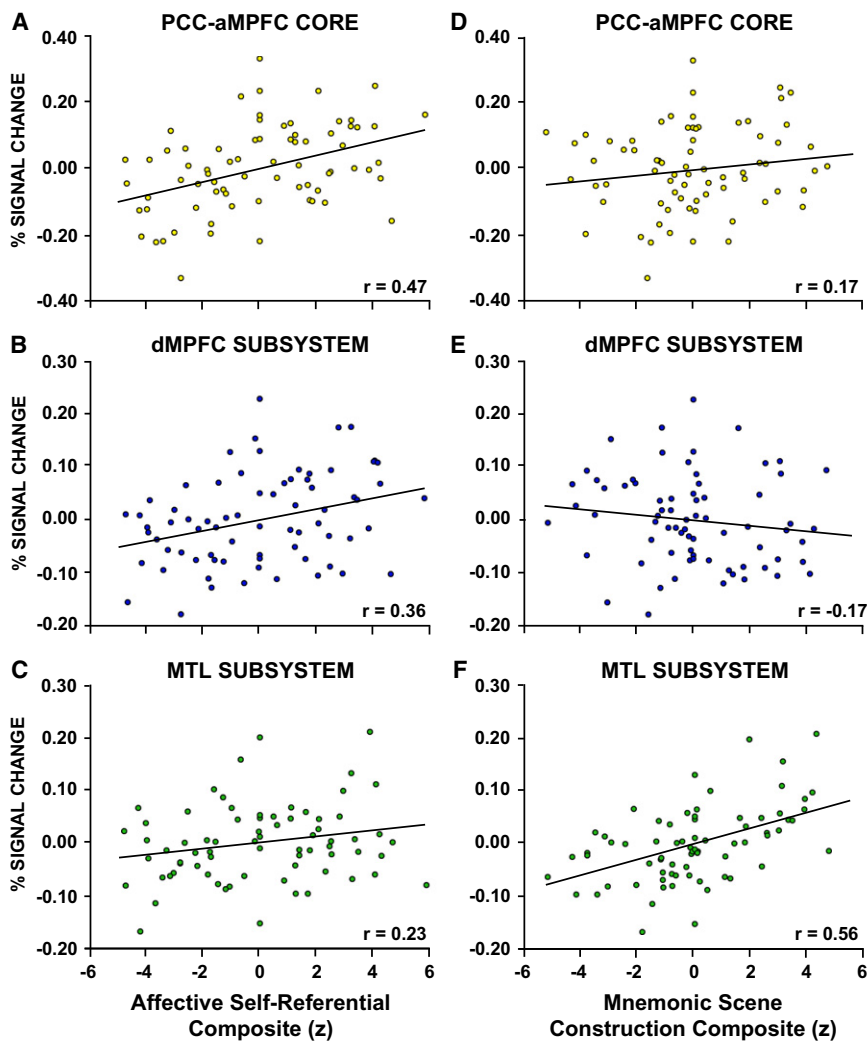
A central observation of the present paper is clear task-based functional dissociation among the components that comprise the default network (Figure 2). In addition, we demonstrate that regions comprising each component show similar patterns of activation. Thus, we extend previous functional accounts by adopting a systems framework.

The MTL subsystem increased its activity preferentially when participants made episodic decisions about their future. This pattern of activity is consistent with a number of functional imaging and neuropsychological studies highlighting the role of the default network in both recall of the past and imagination of the future (reviewed in Schacter et al., 2007). The common

Figure 7. Variance in Activity Accounted for by Composite Measures of Self-Related and Episodic Information

Three variables (personal significance, introspection, and evoked emotion) rated by an independent group of participants for each stimulus were converted to z scores and summed to create a composite measure of affective self-referential cognition. This composite measure was then treated as the independent measure in a linear regression with activity within the (A) PCC-aMPFC core, (B) the dMPFC subsystem, and (C) the MTL subsystem. The affective self-referential composite was found to account for a large portion of the variance in the PCC-aMPFC core (22%) and the dMPFC subsystem (13%), and a small portion of the variance in the MTL subsystem (5%). Next, three additional variables (memory, imagination, and spatial content) were combined into a composite measure of mnemonic scene construction. This composite measure explained a small percentage of the variance in activity within (D) the core (3%) and (E) the dMPFC subsystem (3%), but explained a considerable amount of the variance in activity within (F) the MTL subsystem (31%).

In contrast to the constructive function of the MTL subsystem, the dMPFC subsystem was preferentially active when participants considered their present mental states. Although item analysis was unable to identify specific variables that *selectively* accounted for activity within the dMPFC subsystem, 13% of its variance was accounted for by the affective self-referential composite ($r = 0.36$; $p < 0.005$). These results are consistent with prior studies that report activation of the dMPFC subsystem when information (especially affective information) is referenced to one's self (e.g., Lane et al., 1997; Gusnard et al., 2001; Johnson et al., 2002; Ochsner et al., 2005; Saxe et al., 2006; Vanderwal et al., 2008; Lombardo et al., 2009; reviewed in Ochsner et al., 2004; Amodio and Frith, 2006).

Interestingly, regions within the dMPFC subsystem are also activated when participants infer the mental states of other people (e.g., Gallagher et al., 2000; Saxe and Kanwisher, 2003; Saxe et al., 2006; Ochsner et al., 2005; Lombardo et al., 2009; reviewed in Frith and Frith, 2003; Ochsner et al., 2004; Amodio and Frith, 2006). The possible neural overlap among affective, self-referential, and social cognitive processes suggests a broader role for this subsystem in either metacognition (Ochs-

ner et al., 2004), mental state inference (Frith and Frith, 2003; Olsson and Ochsner, 2008), social cognition (Mitchell, 2006), or the use of one's own mental states as a model for inferring the mental states of others (Goldman, 1992). However, the precise interplay between emotion, self-knowledge, and prediction of other's mental states is still under current investigation, as many stimuli, including those in the present study, confound these processes (see Olsson and Ochsner, 2008, for a review).

Consistent with their possible role in integration as default network hubs, the aMPFC and PCC shared functional properties of both subsystems (Figure 2A), exhibiting preferential self-related activity regardless of temporal context. Additionally, item analyses revealed three variables that correlated with activity in the aMPFC and PCC core: personal significance, introspection about one's own mental states, and evoked emotion (Figure 7). Activity within the aMPFC and PCC is strongest for events that actually happened (Hassabis et al., 2007a), are likely to happen (Szpunar et al., 2009), or are consistent with one's personal future goals (D'Argembeau et al., 2009). Additionally, the aMPFC (and often PCC) activates when participants make judgments or remember trait adjectives about themselves compared to other people (e.g., Kelley et al., 2002; Lou et al., 2004; Heatherton et al., 2006; Mitchell et al., 2006; D'Argembeau et al., 2005) and the regions correlate with self-referential thoughts (D'Argembeau et al., 2005) and perceived similarity or closeness to one's self (Mitchell et al., 2006). These collective observations suggest that the hubs of the default network may

participate in evaluating aspects of personal significance (see also D'Argembeau et al., 2009).

Both Subsystems Are Activated during Passive States, when Participants Engage in Spontaneous Cognition

By exploring the anatomical and functional heterogeneity of the default network using functional connectivity and task-related analyses, we reveal that distinct components of the network contribute differently to internal mentation. What is also novel about the present results is that they suggest why the two subsystems interact when individuals are left to think to themselves undisturbed. Indeed, classic meta-analyses of the default network reveal that a number of regions exhibit greater activity during passive epochs compared to a variety of controlled, externally directed tasks (Shulman et al., 1997; Mazoyer et al., 2001; see also Buckner et al., 2008, 2009; Spreng et al., 2009). The present study suggests that these regions are organized into two distinct subsystems that converge on midline hubs. The joint activation of default network regions during unconstrained passive epochs and experimentally directed tasks emphasizing internal mentation implies an important functional similarity between the two states.

Early reports provided a clue to the nature of this similarity by demonstrating that unconstrained passive states are associated with "freely wandering past recollection, future plans, and other personal thoughts and experiences" (Andreasen et al., 1995; see also Binder et al., 1999; Mazoyer et al., 2001). Along a similar vein, we recently demonstrated a link between spontaneous cognition and default network activity during blocks of fixation, with descriptions indicating that most thoughts were self-relevant and affective in nature (J.R.A.-H. and R.L.B., unpublished data). Thus, when left alone undisturbed, people tend to engage in self-relevant internal cognitive processes predominantly about significant past and future events. These spontaneous cognitive operations likely coactivate multiple distinct subsystems that we have come to know as the default network.

EXPERIMENTAL PROCEDURES

Overview

Three experiments characterized the organization and functions of the default network. Experiment 1 analyzed intrinsic activity correlations between brain regions to determine whether regions form coherent subsystems. Since previous studies have demonstrated that low-frequency spontaneous BOLD correlations between regions largely track direct and indirect anatomical connectivity (reviewed in Fox and Raichle, 2007), experiment 1 was designed to offer insight into the possible anatomical organization of the default network. Two datasets were analyzed for this experiment. The first dataset (n = 28) was used to generate candidate regions within the default network. The second dataset (n = 45) was used to quantify, in an unbiased manner, pairwise correlations between regions. Graph-analytic techniques and hierarchical clustering analyses were then used to determine whether any regions clustered together as components of coherent subsystems.

Experiment 2 explored the functional properties of the core and subsystems using task-based fMRI (n = 46). Subjects made decisions about personal events framed in the context of the present or the future while control questions asked about facts based on semantic knowledge (also referenced to the present or the future). Next, functional magnitudes were extracted on a trial-by-trial basis for each region within the default network followed by hierarchical clustering and correlation analysis to examine functional similarities between regions.

Experiment 3 explored the component processes that tracked activation of the default network subsystems using item analysis and strategy reports. An independent group of subjects (n = 51) were probed in detail about strategies they used for each trial. The answers to the strategy probes were then examined to see which properties, if any, tracked activation of the subsystems and the core that comprise the default network.

Participants

129 right-handed, native English speakers (23.0 years, 18–35, 47 male) recruited from Harvard University, Massachusetts General Hospital, and the greater Boston community participated in at least one of three experiments. 41 of the 129 participants completed both experiment 1, dataset 2 (intrinsic functional connectivity), and experiment 2 (fMRI), bringing the total number of independent data sessions to 170. Demographic information appears in Table S4. Subjects were paid for participation or received course credit. MRI exclusion criteria included history of psychiatric or neurological conditions as well as use of psychoactive medications. Procedures were carried out according to the Partners Health Care Institutional Review Board (experiments 1 and 2) and the Harvard University Committee on the Use of Human Subjects in Research (experiment 3).

MRI Data Acquisition

Scanning was performed on a 3 Tesla Siemens Tim Trio system (Siemens, Erlangen, Germany) using the vendor-supplied 12-channel phased-array head coil. Magnetization prepared rapid acquisition gradient echo (MP-RAGE) 3D T1-weighted anatomical images and T2*-weighted functional data were acquired using procedures outlined in the Supplemental Experimental Procedures. Visual stimuli were programmed using Psychophysics Toolbox software (Brainard, 1997) and were projected onto a computer screen positioned at the back of the scanner. The screen was viewed through an MRI-compatible mirror. Participants wore plastic goggles with either neutral or corrective lenses, were given ear plugs to dampen scanner noise, and used a button box to relay their responses.

Experiment 1: Analysis of Default Network Architecture
Functional Connectivity Preprocessing and Analysis

The goal of the first experiment was to use intrinsic activity correlations to investigate the anatomical heterogeneity within the default network. In an initial dataset (dataset 1), 28 participants (21.0 years, 18–25, 10 male) completed between four and six resting state runs (run duration = 5 min 12 s or 7 min 9 s) comprised of either eyes open fixation, eyes open without fixation, or eyes closed (see Supplemental Experimental Procedures). Default network ROIs were defined in dataset 1 and then examined for clustering properties in an independent test dataset (dataset 2) consisting of 45 participants (21.8 years, 18–30, 17 male) who each completed between two and four fixation runs (run duration = 6 min 30 s). To prepare the MRI data for further analysis, a series of standard preprocessing steps outlined in the Supplemental Experimental Procedures were performed on each dataset (reviewed in Van Dijk et al., 2010).
Definition of Regions

A priori ROIs comprising the default network were defined in dataset 1 and were then used to examine clustering properties in dataset 2. Two initiating, 2 mm radius seed regions were created from a default network meta-analysis of fixation > task data published in Buckner et al. (2009): one near the left PHC (−28, −40, −12) and another within the dMPFC (−4, 48, 24) based on our initial observation of subsystems (Buckner et al., 2008). Several peak coordinates were extracted from the group-averaged correlation maps for the PHC and dMPFC and were converted into 8 mm radii spheres. These regions were then examined for connectivity, and new regions were defined from the subsequent correlation maps. This series of seed and target correlation procedures is similar to those adopted in our previous study (Andrews-Hanna et al., 2007). To simplify the analysis, prevent biasing the structure toward the strong correlations exhibited between mirrored (right/left) seed regions, and to avoid the strong laterality observed for the lateral parietal ROIs (Liu et al., 2009), exclusively left-lateralized ROIs were used resulting in 11 separate left-lateralized or midline regions: dMPFC, aMPFC, vMPFC, pIPL, TPJ, LTC, TempP, PCC, Rsp, PHC, and HF$^+$ (Figures 2A and 2B; Table S1).

Network Analysis

The goal of the network analysis was to determine from the pair-wise regional correlations whether the regions clustered into coherent subsystems (Buckner et al., 2008, 2009). Graph analysis of the pair-wise (11 × 11) correlation matrix was implemented using the "Kamada-Kawai algorithm," a spring-embedded algorithm that pulls connected regions (nodes) together and pushes disconnected regions apart in a manner that minimizes the total energy of the system (Kamada and Kawai, 1989). Betweenness-centrality was used as a quantitative measure of how connected a particular region was to other regions (Freeman, 1977). The z-transformed correlation matrix was then analyzed using a hierarchical-clustering average linkage algorithm (Cluster v3.0, 1988, Stanford University) to provide quantitative evidence for subsystems within the default network. See Supplemental Experimental Procedures for additional details.

Experiment 2: Functional Dissociation among Default Network Subsystems

Experiment 2 sought to dissociate the functional contributions of the default network components isolated from the first experiment by manipulating task demands within an event-related fMRI study. 46 participants (21.7 years, 18–30, 17 male), 41 of whom also participated in the functional connectivity session above (experiment 1, dataset 2), made self-referential or semantic decisions about events framed in the present or the hypothetical future. By manipulating questions that crossed these two factors, we sought to provide clear evidence for task-based functional dissociation.

Task Paradigm

The paradigm was structured using a 2 × 2 design such that questions varied with respect to whether the question was about the participant (Self-Relevancy: *Self* versus *Non-Self Control*) and temporal orientation (*Present* versus *Future*). The goal was to break down component processes that were evoked when individuals imagine themselves in the future (i.e., prospection). The first factor focused on self-relevant processing in contrast to assessments that rely on general semantic knowledge. The second factor focused on the constructive nature of imagined future events by contrasting questions about future events with parallel assessments of the immediate present.

This design yielded four conditions: *Present Self*, *Present Non-Self Control*, *Future Self*, *Future Non-Self Control*. In each of the four conditions, a context-setting statement was made followed by a question. Three possible alternative answers were provided, and subjects responded with a left-handed keypress. Sentence structure, word number, and reading time were matched across the four conditions. Participants were given 10 s to read the contextually orienting sentence and choose their answer. 10 s of fixation separated trials, allowing the hemodynamic response to decay. In this manner, hemodynamic response estimates could be computed for individual trials. A total of 18 trials within each condition were presented across four task runs (72 trials total). Order of trial type was randomized within runs. Additional details are provided in the Supplemental Experimental Procedures.

Following each imaging session, the series of 72 questions was presented to the participants again outside the scanner in a separate behavioral testing room to confirm the experimental conditions differed as expected and to probe the strategies used to answer the questions. Subjects were asked about the various strategies they used to answer each question, including use of mental imagery, vividness, and use of self-projection. Subjects rated imagery by marking the appropriate location along a line between "none" and "a lot." The distance along the line was measured and expressed as a decimal from 1.0 to 10.0, where 1.0 represented "none" and 10.0 represented "a lot." Vividness was rated using the five-point Vividness of Visual Imagery Questionnaire (VVIQ; Marks, 1973). To gauge use of self-projection, participants answered the question "To what degree did you feel like you were there in your image"? by marking the appropriate location along a line between "not at all" or "like it was happening in real life."

Note that many aspects of the scenarios vary from question to question. The four conditions captured broad differences and, as will be illustrated, successfully modulated subsystems within the default network as a function of the 2 × 2 design. However, the variance between individual questions is also relevant. Experiment 3 explicitly explored trial-to-trial variation in the strategies employed to answer the questions by probing the strategies used with an extended set of strategy probes.

Data Processing and Statistical Analyses

A series of preprocessing steps described in the Supplemental Experimental Procedures section were performed on each dataset using SPM2 software (SPM2, Wellcome Trust Center for Neuroimaging, London, UK). In addition to examining contrasts between conditions, item analysis was also employed. As described in the Results section, the group mean percent signal for each trial was correlated between regions within the default network. Pair-wise correlations were then subjected to a hierarchical clustering analysis (used in experiment 1 and described above) that partitions the regions into successively larger clusters based on the similarities of their correlations.

Experiment 3: Functional Analysis of Component Processes

Experiment 3 was conducted to further examine the underlying component processes associated with activity increases across the four task conditions. An independent group of 51 participants (25.2 years, 18–35, 18 male) answered the same set of questions and rated whether they employed different strategies to answer the questions. Their use of strategies was assessed for each individual question using a Likert scale, where 1 represents "not at all" and 7 represents "a lot."

Critically, the three strategy probes employed in experiment 2 were again presented for this independent group of subjects. The answers for these three overlapping questions were strongly correlated between the two subject groups (imagery: r = 0.90; vividness: r = 0.88; self-projection: r = 0.95), suggesting that the present method of probing strategy use captures stable properties of the individual trial questions. Thus, it is reasonable to ascertain strategy assessments in this new group of subjects as a means to understand the fMRI results collected in experiment 2. Eleven new strategy probes were examined (see Table S3 for exact questions), and the mean strategy ratings for each question across the 51 subjects where then used to predict functional activation for each of the items in experiment 2. In this manner, the exact strategies used to make each decision could be examined against fMRI response variance to provide insight into the component processes engaged. Distinct strategies that were similarly employed for each condition were combined into composite measures by summing the z-scores of the individual strategies comprising each composite. Two composites were created: one that included assessment of personal significance (probe #1), introspection about one's preferences, feelings, and emotions (probe #2), and evoked emotion (probe #3), and another that involved use of memory (probe #5), imagination (probe #6), and spatial content (probe #7). Mean activity within the hubs and subsystems separately was correlated with composite scores across participants.

REFERENCES

Addis, D.R., Pan, L., Vu, M.A., Laiser, N., and Schacter, D.L. (2009). Constructive episodic simulation of the future and the past: distinct subsystems of a core brain network mediate imagining and remembering. Neuropsychologia *47*, 2222–2238.

Amodio, D.M., and Frith, C.D. (2006). Meeting of minds: the medial frontal cortex and social cognition. Nat. Rev. Neurosci. *7*, 268–277.

Andreasen, N.C., O'Leary, D.S., Cizadlo, T., Arndt, S., Rezai, K., Watkins, G.L., Ponto, L.L., and Hichwa, R.D. (1995). Remembering the past: two facets of episodic memory explored with positron emission tomography. Am. J. Psychiatry *152*, 1576–1585.

Andrews-Hanna, J.R., Snyder, A.Z., Vincent, J.L., Lustig, C., Head, D., Raichle, M.E., and Buckner, R.L. (2007). Disruption of large-scale brain systems in advanced aging. Neuron *56*, 924–935.

Bar, M. (2007). The proactive brain: using analogies and associations to generate predictions. Trends Cog. Sci. *11*, 280–289.

Barbas, H., Ghashghaei, H., Dombrowski, S.M., and Rempel-Clower, N.L. (1999). Medial prefrontal cortices are unified by common connections with superior temporal cortices and distinguished by input from memory-related areas in the rhesus monkey. J. Comp. Neurol. *410*, 343–367.

Binder, J.R., Frost, J.A., Hammeke, T.A., Bellgowan, P.S., Rao, S.M., and Cox, R.W. (1999). Conceptual processing during the conscious resting state. A functional MRI study. J. Cogn. Neurosci. *11*, 80–93.

Binder, J.R., Desai, R.H., Graves, W.W., and Conant, L.L. (2009). Where is the semantic system? A critical review and meta-analysis of 120 functional neuroimaging studies. Cereb. Cortex *19*, 2767–2796.

Brainard, D.H. (1997). The psychophysics toolbox. Spat. Vis. *10*, 433–436.

Broyd, S.J., Demanuele, C., Debener, S., Helps, S.K., James, C.J., and Sonuga-Barke, E.J. (2009). Default-mode brain dysfunction in mental disorders: a systematic review. Neurosci. Biobehav. Rev. *33*, 279–296.

Buckner, R.L., Andrews-Hanna, J.R., and Schacter, D.L. (2008). The brain's default network: anatomy, function, and relevance to disease. Ann. N Y Acad. Sci. *1124*, 1–38.

Buckner, R.L., Sepulcre, J., Talukdar, T., Krienen, F.M., Liu, H., Hedden, T., Andrews-Hanna, J.R., Sperling, R.A., and Johnson, K.A. (2009). Cortical hubs revealed by intrinsic functional connectivity: mapping, assessment of stability, and relation to Alzheimer's disease. J. Neurosci. *29*, 1860–1873.

Christoff, K., Gordon, A.M., Smallwood, J., Smith, R., and Schooler, J.W. (2009). Experience sampling during fMRI reveals default network and executive system contributions to mind wandering. Proc. Natl. Acad. Sci. USA *106*, 8719–8724.

D'Argembeau, A., Collette, F., Van der Linden, M., Laureys, S., Del Fiore, G., Degueldre, C., Luxen, A., and Salmon, E. (2005). Self-referential reflective activity and its relationship with rest: a PET study. Neuroimage *25*, 616–624.

D'Argembeau, A., Stawarczyk, D., Majerus, S., Collette, F., Van der Linden, M., Feyers, D., Maquet, P., and Salmon, E. (2009). The neural basis of personal goal processing when envisioning future events. J. Cogn. Neurosci., in press. Published online July 30, 2009. 10.1162/jocn.2009.21314.

Fox, M.D., and Raichle, M.E. (2007). Spontaneous fluctuations in brain activity observed with functional magnetic resonance imaging. Nat. Rev. Neurosci. *8*, 700–711.

Fransson, P., and Marrelec, G. (2008). The precuneus/posterior cingulate cortex plays a pivotal role in the default mode network: Evidence from a partial correlation network analysis. Neuroimage *42*, 1178–1184.

Freeman, L.C. (1977). A set of measures of centrality based on betweenness. Sociometry *40*, 35–41.

Frith, U., and Frith, C.D. (2003). Development and neurophysiology of mentalizing. Philos. Trans. R. Soc. Lond. B Biol. Sci. *358*, 459–473.

Gallagher, H.L., Happé, F., Brunswick, N., Fletcher, P.C., Frith, U., and Frith, C.D. (2000). Reading the mind in cartoons and stories: an fMRI study of 'theory of mind' in verbal and nonverbal tasks. Neuropsychologia *38*, 11–21.

Gilbert, S.J., Dumontheil, I., Simons, J.S., Frith, C.D., and Burgess, P.W. (2007). Comment on "Wandering minds: the default network and stimulus-independent thought". Science *317*, 43.

Goldman, A.I. (1992). In defense of the simulation theory. Mind Lang. *7*, 104–119.

Gollwitzer, P.M., and Brandstätter, V. (1997). Implementation intentions and effective goal pursuit. J. Pers. Soc. Psychol. *73*, 186–199.

Greicius, M.D., Srivastava, G., Reiss, A.L., and Menon, V. (2004). Default-mode network activity distinguishes Alzheimer's disease from healthy aging: evidence from functional MRI. Proc. Natl. Acad. Sci. USA *101*, 4637–4642.

Gusnard, D.A., and Raichle, M.E. (2001). Searching for a baseline: functional imaging and the resting human brain. Nat. Rev. Neurosci. *2*, 685–694.

Gusnard, D.A., Akbudak, E., Shulman, G.L., and Raichle, M.E. (2001). Medial prefrontal cortex and self-referential mental activity: relation to a default mode of brain function. Proc. Natl. Acad. Sci. USA *98*, 4259–4264.

Hagmann, P., Cammoun, L., Gigandet, X., Meuli, R., Honey, C.J., Wedeen, V.J., and Sporns, O. (2008). Mapping the structural core of human cerebral cortex. PLoS Biol. *6*, e159.

Hassabis, D., and Maguire, E.A. (2007). Deconstructing episodic memory with construction. Trends Cogn. Sci. *11*, 299–306.

Hassabis, D., Kumaran, D., and Maguire, E.A. (2007a). Using imagination to understand the neural basis of episodic memory. J. Neurosci. *27*, 14365–14374.

Hassabis, D., Kumaran, D., Vann, S.D., and Maguire, E.A. (2007b). Patients with hippocampal amnesia cannot imagine new experiences. Proc. Natl. Acad. Sci. USA *104*, 1726–1731.

Heatherton, T.F., Wyland, C.L., Macrae, C.N., Demos, K.E., Denny, B.T., and Kelley, W.M. (2006). Medial prefrontal activity differentiates self from close others. Soc. Cogn. Affect. Neurosci. *1*, 18–25.

James, W. (1890). The Principles of Psychology (New York: Henry Holt and Company).

Johnson, S.C., Baxter, L.C., Wilder, L.S., Pipe, J.G., Heiserman, J.E., and Prigatano, G.P. (2002). Neural correlates of self-reflection. Brain *125*, 1808–1814.

Kahn, I., Andrews-Hanna, J.R., Vincent, J.L., Snyder, A.Z., and Buckner, R.L. (2008). Distinct cortical anatomy linked to subregions of the medial temporal lobe revealed by intrinsic functional connectivity. J. Neurophysiol. *100*, 129–139.

Kamada, T., and Kawai, S. (1989). An algorithm for drawing general undirected graphs. Inf. Process. Lett. *31*, 7–15.

Kelley, W.M., Macrae, C.N., Wyland, C.L., Caglar, S., Inati, S., and Heatherton, T.F. (2002). Finding the self? An event-related fMRI study. J. Cogn. Neurosci. *14*, 785–794.

Klinger, E. (1971). Structure and Functions of Fantasy (New York: John Wiley and Sons, Inc).

Klinger, E., and Cox, W.M. (1987). Dimensions of thought flow in everyday life. Imagin. Cogn. Pers. *7*, 105–128.

Kobayashi, Y., and Amaral, D.G. (2003). Macaque monkey retrosplenial cortex: II. Cortical afferents. J. Comp. Neurol. *466*, 48–79.

Kobayashi, Y., and Amaral, D.G. (2007). Macaque monkey retrosplenial cortex: III. Cortical efferents. J. Comp. Neurol. *502*, 810–833.

Kondo, H., Saleem, K.S., and Price, J.L. (2005). Differential connections of the perirhinal and parahippocampal cortex with the orbital and medial prefrontal networks in macaque monkeys. J. Comp. Neurol. *493*, 479–509.

Lane, R.D., Fink, G.R., Chau, P.M.-L., and Dolan, R.J. (1997). Neural activation during selective attention to subjective emotional responses. Neuroreport *8*, 3969–3972.

Lavenex, P., Suzuki, W.A., and Amaral, D.G. (2002). Perirhinal and parahippocampal cortices of the macaque monkey: projections to the neocortex. J. Comp. Neurol. *447*, 394–420.

Liu, H., Stufflebeam, S.M., Sepulcre, J., Hedden, T., and Buckner, R.L. (2009). Evidence from intrinsic activity that asymmetry of the human brain is controlled by multiple factors. Proc. Natl. Acad. Sci. USA *106*, 20499–20503.

Lombardo, M.V., Chakrabarti, B., Bullmore, E.T., Wheelright, S.J., Sadek, S.A., Suckling, J., MRC AIMS Consortium, and Baron-Cohen, S. (2009). Shared neural ciruits for mentalizing about the self and others. J. Cogn. Neurosci., in press. Published online July 6, 2009. 10.1162/jocn.2009.21287.

Lou, H.C., Luber, B., Crupain, M., Keenan, J.P., Nowak, M., Kjaer, T.W., Sackeim, H.A., and Lisanby, S.H. (2004). Parietal cortex and representation of the mental Self. Proc. Natl. Acad. Sci. USA *101*, 6827–6832.

Margulies, D.S., Kelly, A.M., Uddin, L.Q., Biswal, B.B., Castellanos, F.X., and Milham, M.P. (2007). Mapping the functional connectivity of anterior cingulate cortex. Neuroimage *37*, 579–588.

Margulies, D.S., Vincent, J.L., Kelly, C., Lohmann, G., Uddin, L.Q., Biswal, B.B., Villringer, A., Castellanos, F.X., Milham, M.P., and Petrides, M. (2009). Precuneus shares intrinsic functional architecture in humans and monkeys. Proc. Natl. Acad. Sci. USA *106*, 20069–20074.

Marks, D.F. (1973). Visual imagery differences in the recall of pictures. Br. J. Psychol. *64*, 17–24.

Mason, M.F., Norton, M.I., Van Horn, J.D., Wegner, D.M., Grafton, S.T., and Macrae, C.N. (2007). Wandering minds: the default network and stimulus-independent thought. Science *315*, 393–395.

Mazoyer, B., Zago, L., Mellet, E., Bricogne, S., Etard, O., Houdé, O., Crivello, F., Joliot, M., Petit, L., and Tzourio-Mazoyer, N. (2001). Cortical networks for working memory and executive functions sustain the conscious resting state in man. Brain Res. Bull. *54*, 287–298.

McKiernan, K.A., Kaufman, J.N., Kucera-Thompson, J., and Binder, J.R. (2003). A parametric manipulation of factors affecting task-induced deactivation in functional neuroimaging. J. Cogn. Neurosci. *15*, 394–408.

McKiernan, K.A., D'Angelo, B.R., Kaufman, J.N., and Binder, J.R. (2006). Interrupting the "stream of consciousness": an fMRI investigation. Neuroimage *29*, 1185–1191.

Mitchell, J.P. (2006). Mentalizing and Marr: an information processing approach to the study of social cognition. Brain Res. *1079*, 66–75.

Mitchell, J.P., Macrae, C.N., and Banaji, M.R. (2006). Dissociable medial prefrontal contributions to judgments of similar and dissimilar others. Neuron *50*, 655–663.

Morcom, A.M., and Fletcher, P.C. (2007). Does the brain have a baseline? Why we should be resisting a rest. Neuroimage *37*, 1073–1082.

Morecraft, R.J., Cipolloni, P.B., Stilwell-Morecrat, K.S., Gedney, M.T., and Pandya, D.N. (2004). Cytoarchitecture and cortical connections of the posterior cingulate and adjacent somatosensory fields in the rhesus monkey. J. Comp. Neurol. *469*, 37–69.

Ochsner, K.N., Knierim, K., Ludlow, D.H., Hanelin, J., Ramachandran, T., Glover, G., and Mackey, S.C. (2004). Reflecting upon feelings: an fMRI study of neural systems supporting the attribution of emotion to self and other. J. Cogn. Neurosci. *16*, 1746–1772.

Ochsner, K.N., Beer, J.S., Robertson, E.R., Cooper, J.C., Gabrieli, J.D.E., Kihlstrom, J.F., and D'Esposito, M. (2005). The neural correlates of directed and reflected self-knowledge. Neuroimage *28*, 797–814.

Olsson, A., and Ochsner, K.N. (2008). The role of social cognition in emotion. Trends Cogn. Sci. *12*, 65–71.

Price, J.L. (2007). Definition of the orbital cortex in relation to specific connections with limbic and visceral structures and other cortical regions. Ann. N Y Acad. Sci. *1121*, 54–71.

Raichle, M.E., MacLeod, A.M., Snyder, A.Z., Powers, W.J., Gusnard, D.A., and Shulman, G.L. (2001). A default mode of brain function. Proc. Natl. Acad. Sci. USA *98*, 676–682.

Saxe, R., and Kanwisher, N. (2003). People thinking about thinking people. The role of the temporo-parietal junction in "theory of mind". Neuroimage *19*, 1835–1842.

Saxe, R., Moran, J.M., Scholz, J.E., and Gabrieli, J. (2006). Overlapping and non-overlapping brain regions for theory of mind and self reflection in individual subjects. Soc. Cogn. Affect. Neurosci. *1*, 229–234.

Schacter, D.L., and Addis, D.R. (2007). The cognitive neuroscience of constructive memory: remembering the past and imagining the future. Philos. Trans. R. Soc. Lond. B Biol. Sci. *362*, 773–786.

Schacter, D.L., Addis, D.R., and Buckner, R.L. (2007). Remembering the past to imagine the future: the prospective brain. Nat. Rev. Neurosci. *8*, 657–661.

Schilbach, L., Eickhoff, S.B., Rotarska-Jagiela, A., Fink, G.R., and Vogeley, K. (2008). Minds at rest? Social cognition as the default mode of cognizing and its putative relationship to the "default system" of the brain. Conscious. Cogn. *17*, 457–467.

Shulman, G.L., Fiez, J.A., Corbetta, M., Buckner, R.L., Miezen, F.M., Raichle, M.E., and Petersen, S.E. (1997). Common blood flow changes across visual tasks: II: decreases in cerebral cortex. J. Cogn. Neurosci. *9*, 648–663.

Singer, J.L. (1966). Daydreaming: An Introduction to the Experimental Study of Inner Experience (New York: Random House, Inc).

Spreng, R.N., Mar, R.A., and Kim, A.S. (2009). The common neural basis of autobiographical memory, prospection, navigation, theory of mind, and the default mode: a quantitative meta-analysis. J. Cogn. Neurosci. *21*, 489–510.

Suzuki, W.A., and Amaral, D.G. (1994). Perirhinal and parahippocampal cortices of the macaque monkey: cortical afferents. J. Comp. Neurol. *350*, 497–533.

Szpunar, K.K., Chan, J.C., and McDermott, K.B. (2009). Contextual processing in episodic future thought. Cereb. Cortex *19*, 1539–1548.

Van Dijk, K.R., Hedden, T., Venkataraman, A., Evans, K.C., Lazar, S.W., and Buckner, R.L. (2010). Intrinsic functional connectivity as a tool for human connectomics: theory, properties, and optimization. J. Neurophysiol. *103*, 297–321.

Van Essen, D.C. (2005). A Population-Average, Landmark- and Surface-based (PALS) atlas of human cerebral cortex. Neuroimage *28*, 635–662.

Vanderwal, T., Hunyadi, E., Grupe, D.W., Connors, C.M., and Schultz, R.T. (2008). Self, mother and abstract other: an fMRI study of reflective social processing. Neuroimage *41*, 1437–1446.

Vincent, J.L., Snyder, A.Z., Fox, M.D., Shannon, B.J., Andrews, J.R., Raichle, M.E., and Buckner, R.L. (2006). Coherent spontaneous activity identifies a hippocampal-parietal memory network. J. Neurophysiol. *96*, 3517–3531.

Wicker, B., Ruby, P., Royet, J.P., and Fonlupt, P. (2003). A relation between rest and the self in the brain? Brain Res. Rev. *43*, 224–230.